

January 01, 2007

The Complete Electrode Model for Imaging and Electrode Contact Compensation in Electrical Impedance Tomography

Greg Boverman
Rensselaer Polytechnic Institute

B. S. Kim
Rensselaer Polytechnic Institute

Tzu-Jen Kao
Rensselaer Polytechnic Institute

David Isaacson
Rensselaer Polytechnic Institute

Gary J. Saulnier
Rensselaer Polytechnic Institute

See next page for additional authors

Recommended Citation

Boverman, Greg; Kim, B. S.; Kao, Tzu-Jen; Isaacson, David; Saulnier, Gary J.; and Newell, Jonathan C., "The Complete Electrode Model for Imaging and Electrode Contact Compensation in Electrical Impedance Tomography" (2007). *Research Thrust R2 Presentations*. Paper 41. <http://hdl.handle.net/2047/d10008810>

Author(s)

Greg Boverman, B. S. Kim, Tzu-Jen Kao, David Isaacson, Gary J. Saulnier, and Jonathan C. Newell



THE COMPLETE ELECTRODE MODEL FOR IMAGING AND ELECTRODE CONTACT COMPENSATION IN ELECTRICAL IMPEDANCE TOMOGRAPHY

G. Boverman¹, B.S. Kim¹, T.-J. Kao³, D. Isaacson², G.J. Saulnier³, and J.C. Newell¹

Departments of ¹Biomedical Engineering, ²Mathematical Sciences, and ³Electrical, Computer and Systems Engineering, Rensselaer Polytechnic Institute, Troy, NY



Introduction:

Electrical Impedance Tomography (EIT) is an imaging modality which currently shows promise for the detection and characterization of breast cancer. A very significant problem in EIT imaging is the proper modeling of the interface between the body and the electrodes. We have found empirically that it is very difficult, in a clinical setting, to assure that all electrodes make satisfactory contact with the body. In addition, we have observed a capacitive effect at the skin/electrode boundary that is spatially heterogeneous. To compensate for these problems, we have developed a hybrid nonlinear-linear reconstruction algorithm in which we first estimate electrode surface impedances, using a Newton-type iterative optimization procedure with an analytically compute Jacobian matrix. We subsequently make use of a linearized algorithm to perform a three-dimensional reconstruction of perturbations in both contact impedances and in the spatial distributions of conductivity and permittivity.

Results show that, using this procedure, artifacts due to electrodes making poor contact can be greatly reduced.

EIT and Tomosynthesis co-registered

The ACT 4 system [1] is the electrical impedance imaging system being developed at Rensselaer. It is a high-speed, high-precision, multi-frequency, multi-channel instrument which supports 64 channels and electrodes. Each electrode is driven by a high precision voltage source, and has a circuit for measuring the resulting electrode current. These circuits are digitally controlled to produce and measure signals at 5k, 10k, 30k, 100k, 300k and 1MHz. The magnitude and phase of each source are controlled independently.

The system has been used to study breast cancer patients at Massachusetts General Hospital in conjunction with a tomosynthesis machine and verified with biopsy results. The EIT images are co-registered with tomosynthesis images since the EIT electrodes are placed on the mammograph plates as shown.

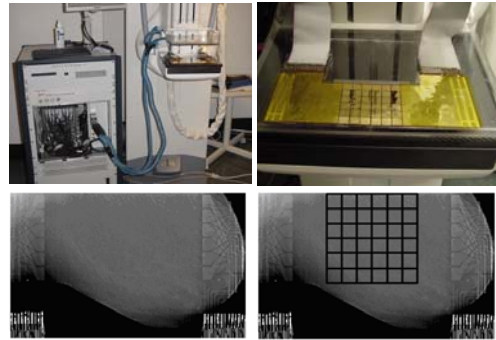


Figure 1. ACT 4 with the mammography unit (top left), radiolucent electrode array [2] attached to the lower compression plate (upper right), one slice of the tomosynthesis image made with the electrode arrays in place of the left breast from human subject HS14 (lower left) and tomosynthesis image with an overlaid grid showing the location of the active electrode surfaces (lower right). Note that the copper leads and ribbon cables are visible on the left and right of the tomosynthesis images but the radiolucent portion of the arrays is not visible.

Idealized Model of Breast Geometry:

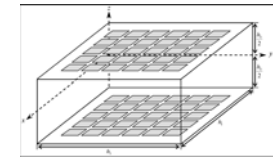


Figure 2. The mammography geometry is modeled as a rectangular box with electrodes on the top and bottom planes.

Mathematical Formulation of the Complete Electrode Model:

In the quasi-static approximation of Maxwell's equations, the potential within the body is governed by the following equation:

$$\nabla \cdot \gamma \nabla u(p) = 0, \text{ for } p \text{ in } \Omega. \quad (1)$$

We use a series eigenfunction decomposition of the potential:

$$u(x, y, z) = b_0 z + \sum_{m=1}^N \sum_{n=1}^N a_{n,m} \cos(\lambda_n x) \cos(\lambda_m y) \cosh(\lambda_{n,m} z) + b_{n,m} \cos(\lambda_n x) \cos(\lambda_m y) \sinh(\lambda_{n,m} z)$$

$$\lambda_n = \frac{n\pi}{h_1}, \lambda_m = \frac{m\pi}{h_2}, \lambda_{n,m} = \sqrt{\lambda_n^2 + \lambda_m^2}$$

The complete electrode model (CEM) specifies a set of boundary conditions for Eq. 1 that have been experimentally shown to be accurate in modeling the interface between highly conductive electrodes and a considerably less conductive medium. First of all, we know the total current injected through each electrode, and we assume that no current flows out through regions of the surface where electrodes are not present:

$$\int_{\epsilon_\ell} \gamma \frac{\partial u(p)}{\partial \nu} dS = I_\ell \text{ on } \epsilon_\ell, \ell = 1, 2, \dots, L$$

$$\gamma \frac{\partial u(p)}{\partial \nu} = 0 \text{ off } \bigcup_{\ell=1}^L \epsilon_\ell$$

$$u(p) + z_\ell \gamma \frac{\partial u(p)}{\partial \nu} = U_\ell \text{ on } \epsilon_\ell, \ell = 1, 2, \dots, L$$

$$\sum_{\ell=1}^L U_\ell = 0$$

$$\sum_{\ell=1}^L I_\ell = 0$$

In implementing the complete model, we make use of a Galerkin approach, in which, we have the condition that, for each test function, v , the following equation must be satisfied:

$$\int_{\Omega} v \nabla \cdot \gamma \nabla u dp = 0.$$

Using the divergence theorem and applying the conditions of the CEM, we then find:

$$\int_{\Omega} \gamma \nabla u \cdot \nabla v dp + \sum_{\ell=1}^L \frac{1}{z_\ell} \left[\int_{\epsilon_\ell} uv dS - \frac{1}{|\epsilon_\ell|} \int_{\epsilon_\ell} u dS \int_{\epsilon_\ell} v dS \right] = \sum_{\ell=1}^L \frac{I_\ell}{|\epsilon_\ell|} \int_{\epsilon_\ell} v dS.$$

Linearization and Reconstruction

Using the divergence theorem applied to Eq. 1, we find that, for the potentials due to two current patterns

$$\int_{\Omega} \gamma \nabla u^{\alpha}(\mathbf{x}, \gamma) \cdot \frac{\partial u^{\beta}(\mathbf{x}, \gamma)}{\partial \nu} dS = \int_{\Omega} (\gamma - \gamma_0) \nabla u^{\alpha}(\mathbf{x}, \gamma) \cdot \nabla u^{\beta}(\mathbf{x}, \gamma) dV$$

$$D \approx \mathbf{J}_z \delta z + \mathbf{J}_\gamma \delta \gamma$$

$$\sum_{\ell=1}^L (U_\ell^{\alpha} I_\ell^{\beta} - U_\ell^{\beta} I_\ell^{\alpha}) - \sum_{\ell=1}^L \int_{\epsilon_\ell} \gamma_0 \delta z \frac{\partial u^{\alpha}(\mathbf{x}, \gamma)}{\partial \nu} \frac{\partial u^{\beta}(\mathbf{x}, \gamma)}{\partial \nu} dS = \int_{\Omega} (\gamma - \gamma_0) \nabla u^{\alpha}(\mathbf{x}, \gamma) \cdot \nabla u^{\beta}(\mathbf{x}, \gamma) dV$$

$$\mathbf{J}_{\gamma_n}^{\alpha, \beta} = \int_{\Omega} \nabla u^{\alpha}(\mathbf{x}, \gamma_0) \cdot \nabla u^{\beta}(\mathbf{x}, \gamma_0) dV$$

$$\mathbf{J}_{z_\ell}^{\alpha, \beta} = \int_{\epsilon_\ell} \gamma_0 \frac{\partial u^{\alpha}(\mathbf{x}, \gamma_0)}{\partial \nu} \frac{\partial u^{\beta}(\mathbf{x}, \gamma_0)}{\partial \nu} dS$$

Phantom Experiments:

We tested the methods presented in this poster using a breast-shaped phantom:

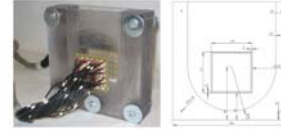


Figure 3. The 60-electrode test phantom for the 3-D mammography geometry used in the experiments.

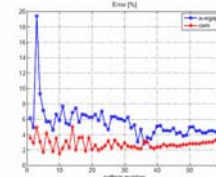


Figure 4. Relative norm error for the ave-gap and complete electrode models (saline tank).

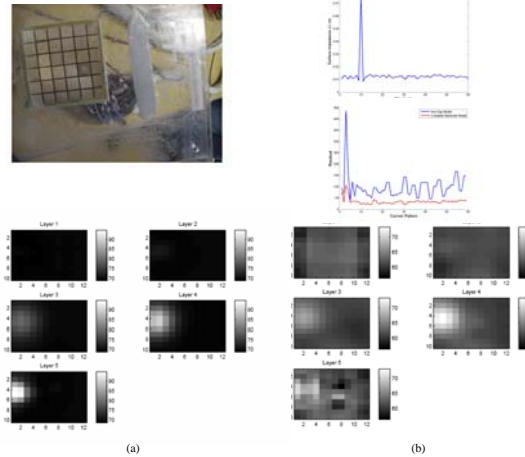


Figure 5. Compensation for a poorly contacting electrode using the CEM. (a) Difference imaging reconstruction (for reference). (b) Reconstruction using the CEM and estimated surface impedances.

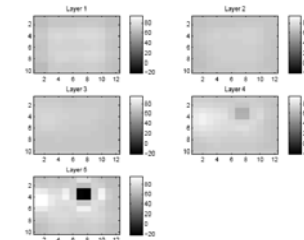


Figure 6. Reconstruction using an ave-gap model.

Application to Clinical Data:

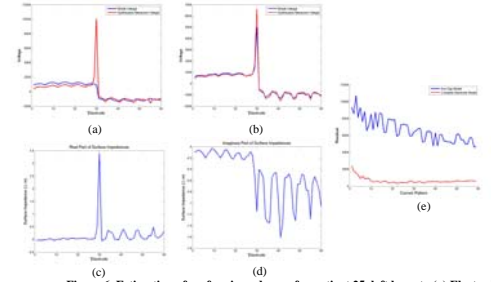
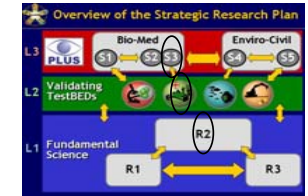


Figure 6. Estimation of surface impedances for patient 25, left breast. (a) Electrode test for ave-gap model. (b) Electrode test for CEM. (c) Real part of estimated surface impedances. (d) Imaginary part of estimated surface impedances. (e) Reduction in residual using the CEM and estimated surface impedances.

Importance of the work and technology transfer:

The EIT clinical data and analysis in mammogram geometry provide a foundation to assess the value of EIT as an adjunct to mammography for breast cancer screening and diagnosis.



This work is supported in part by CnSSIS, the Center for Subsurface Sensing and Imaging Systems, under the Engineering Research Centers Program of the National Science Foundation (Award Number EEC-9986821) and by NIBIB, the National Institute of Biomedical Imaging and Bioengineering under Grant Number R01-EB000456-03.

References:

Publications Acknowledging NSF Support:

1. Ning Liu, Gary J. Saulnier, J.C. Newell, D. Isaacson and T-J Kao. "ACT4: A High-Precision, Multi-Frequency Electrical Impedance Tomography" Conference on Biomedical Applications of Electrical Impedance Tomography, University College London, June 22-24th, 2005.
2. Choi, M.H., T-J. Kao, D. Isaacson, G.J. Saulnier and J.C. Newell "A Reconstruction Algorithm for Breast Cancer Imaging with Electrical Impedance Tomography in Mammography Geometry" IEEE Trans. Biomed. Eng. 54(4), 2007.
3. Kim, B.S., G. Boverman, J. C. Newell, G.J. Saulnier, and D. Isaacson "The Complete Electrode Model for EIT in a Mammography Geometry" Physiol. Meas. 2007 (in Press).
4. Boverman, G., B.S. Kim, D. Isaacson, and J.C. Newell. "The Complete Electrode Model for Modeling and Electrode Contact Compensation in Electrical Impedance Tomography", submitted to the IEEE EMSB Conference, 2007.

Others:

1. T. Vihunen, J. P. Kaipio, P. J. Vauhkonen, T. Savolainen, and M. Vauhkonen, "Simultaneous reconstruction of electrode contact impedances and internal electrical properties: I. Theory." Meas. Sci. Technol., 13, 2002.

Contact Info:

Jonathan Newell, Ph. D. Research Professor of Biomedical Engineering
E-mail: newell@rpi.edu Rensselaer Polytechnic Institute
Web site: http://www.rpi.edu/~newell/eit.html

110 Eighth St. Troy, NY 12180-3590
Phone : 518-276-6433 FAX : 518-276-3035

